

A Fairness–Throughput Tradeoff Perspective on NOMA Multiresolution Broadcasting

Adriano Pastore, *Member, IEEE*, and Monica Navarro, *Member, IEEE*

Abstract—We propose an analytical framework for characterizing the tradeoff between fairness and throughput that arises in a cellular or satellite downlink when multicast information is encoded in two resolution levels (high vs. low priority information). Given a target fairness (measured in terms of the ratio between the information rates of low vs. high resolution stream), the operator seeks to optimize the modulation and coding schemes so as to maximize the average cell throughput. Viewing operating points as fairness–throughput pairs allows to meaningfully quantify and interpret the superiority of non-orthogonal (NOMA) techniques such as superposition coding against simple orthogonal time division. The optimal fairness–throughput tradeoff curve for superposition coding vs. time division is derived in the Gaussian setting. A practical implementation with 16-QAM constellations and multilevel coding is proposed and its tradeoff curve is numerically evaluated.

Index Terms—broadcast, multiresolution, multilevel coding, fairness, Non-Orthogonal Multiple Access (NOMA), Orthogonal Multiple Access (OMA).

I. INTRODUCTION

SERVING as a model for most downlink channels, the information-theoretic broadcast channel, in which K private messages are conveyed by a common transmitter to K receivers, was introduced by Cover [1]. Its capacity is only known to day in some special cases—most notably, for the case of degraded channels [2], in which superposition coding is known to achieve capacity [3], or for the case of vector Gaussian channels [4] using dirty-paper coding.

In contrast to this private-message broadcast channel, in the *multiresolution broadcast channel*, there exist multiple messages that have to be conveyed to different *subsets* of receivers. Specifically, we refer to the multiresolution broadcasting problem with two resolution levels as one where a common message (low-resolution information) has to be reliably decoded by all receivers, whereas an optional message (refinement information to resolve for higher resolution) ought to be decoded by an arbitrary (non-empty) subset of users. From an applications perspective, the information conveyed in such manner can consist of multicast messages such as, for example, a live stream or cached multimedia content (television, video stream, radio program, etc.) that comes in a high and a low quality version. A complete information-theoretic characterization of the multiresolution capacity region is still missing, but some important advances have been recently reported in [5].

If a single level of quality of service (QoS) is enforced for all users, then the maximum rate at which all users can reliably decode the message will be fundamentally limited by the user with the worst channel, i.e., the user with lowest single-user capacity, which in cellular systems is typically located at the

cell edge. Provided that we allow some QoS diversity—as in the example of high-definition vs. low-definition scalable video streaming—this limitation can be lifted. In fact, backing off from perfect QoS fairness allows the broadcasting operator to deliver a higher-quality service to some subscribers and typically achieve a higher sum throughput (collective utility). In this operating mode, users experiencing poor channel conditions will decode a coarse, low resolution version of the information, whereas users with a stronger channel will additionally decode refinement information to resolve for a higher resolution version. Clearly, this problem can be generalized to more than two resolution levels, but we will only be concerned with two levels in this article.

A simple handle on balancing QoS diversity in this context could be to apply an Orthogonal Multiple Access (OMA) scheme, whereby the coarse (high-priority) and refinement (low-priority) information would be assigned to orthogonal resources. For example, one could apply time division multiplexing (TDM) for this purpose. However, non-orthogonal schemes such as power-domain multiplexing—which are known [6] to outperform their orthogonal counterparts—are currently receiving increased attention as a promising way to improve efficiency and flexibility of cellular or satellite communication systems. One example is the adoption by 3GPP of Multi-User Superposition Transmission (MUST) [7]. This scheme has also been referred to as Non-Orthogonal Multiple Access (NOMA) and is known to improve throughput performance by means of superposition coding, suitable power allocation and successive interference cancellation at the receiver. Theoretical results further demonstrate that practical implementations of superposition schemes such as multilevel coded modulation (MLC) can achieve higher rates than orthogonal schemes [8]. The authors of [9] propose a framework for NOMA broadcasting based on both binary component channel decomposition and non-binary constituent codes, offering guidelines for the selection of the substream rates, practical transceiver implementations and flexible designs. A comprehensive survey of several candidate NOMA schemes for fifth-generation (5G) cellular networks can be found in [10].

Regarding the multiresolution broadcast problem specifically, Layered Division Multiplexing (LDM) has been proposed for digital terrestrial broadcasting [11], [12]. The recent publication [13] provides a detailed study of the capacity advantage of LDM over orthogonal schemes for multi-tier (in our terminology: multiresolution) service delivery and mixed unicast–broadcast service delivery.

The main focus of [13], however, is not on fairness issues. On the other hand, [14] is closest in spirit to our work, in that it studies max-min fairness optimization in a NOMA downlink.

However, the crucial difference is that it is concerned with the private-message broadcast channel: fairness considerations from private-message broadcasting, however, do not carry over to multiresolution broadcasting. In particular, the general trend that we will observe for the NOMA scheme—in which average throughput, as a function of fairness, exhibits a maximum—does not manifest in the private-message setting. It is important to remark that the multiresolution broadcast channel also differs from the so-called broadcast channel with a *common message* and the broadcast channel with *degraded message sets*, first studied in [15], despite strong similarities and connections. Although said settings have attracted more attention in information-theoretic studies, their capacity regions are only known in few special cases. Even in the case of mutually degraded channel laws, superposition coding is known to be suboptimal [16] in general. Other work such as [17], [18] provide insight into optimal schemes without fully solving the problem.

One central aspect when devising practical downlink schemes is the fact that, in private-message and multiresolution broadcasting alike, fairness and throughput are inherently conflicting objectives. This already becomes apparent in the simplest two-user Gaussian broadcast channel capacity [19, Sec. 5.5.1], in which the sum-rate maximizing strategy consists in allocating all power to the stronger user. Fairness-enforcing strategies will generally chip away at the overall throughput performance. Traditionally, in cellular systems with orthogonal transmission, the question of fairness has been addressed by resource allocation (scheduling, beam selection, etc.). By contrast, in NOMA schemes, the question of fairness arises more fundamentally in the design of the coding scheme itself. Recent works have addressed optimization in NOMA downlink systems [14], [20]. In [21], Jain's fairness index [22] is considered to compare OMA and NOMA approaches for the uplink multiple access channel. In this paper, which to the best of our knowledge is the first to consider the fairness issue in NOMA multiresolution broadcasting, we base our fairness metric on the ratio between the QoS levels respectively associated to the low-resolution vs. high-resolution version of the information stream, whereas the utility metric is associated to the average system throughput. Given the diversity of signal-to-noise ratios ensuing from the randomness of user locations, the choice is between delivering high-resolution information to a few, or low-resolution information to many. In this work, we propose a framework to characterize this fairness–utility tradeoff.

II. FAIRNESS AND UTILITY

Consider a multi-user communication system serving K users. We seek to characterize a tradeoff between *user fairness* and a collective *utility* metric based on a notion of quality of service. Suppose Q_k denotes some (non-negative) measure of quality of service (QoS) experienced by user $k \in \{1, \dots, K\}$. We define the *fairness* F as the ratio

$$F \triangleq \frac{\min\{Q_1, \dots, Q_K\}}{\max\{Q_1, \dots, Q_K\}} \quad (1)$$

and the (average) *utility* U as the quantity

$$U \triangleq \frac{1}{K} \sum_k g(Q_k) \quad (2)$$

where g is some monotone non-negative function which may model any sort of per-user benefit (e.g., probability of successful decoding, user satisfaction or perceived quality of service, customer pricing or marginal revenue for the operator, etc.). In this abstract formulation, the tradeoff problem consists in characterizing the outer boundary of the set of jointly feasible fairness–utility pairs (F, U) by varying over all admissible encoding and decoding schemes.

In this article, we will focus on a multiresolution downlink channel. We will assimilate the QoS quantities Q_k to the reliably decodable information rates R_k and restrict g to the identity function. Hence F will represent rate fairness, while U will represent the average cell throughput.

III. THE MULTIRESOLUTION BROADCAST CHANNEL

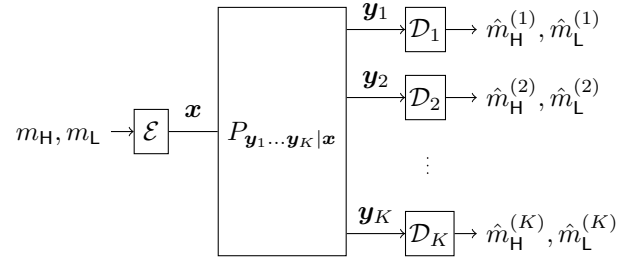


Fig. 1. A K -user multiresolution broadcast channel with two resolution levels (high- and low-priority layer)

Consider the multiresolution broadcast channel as depicted in Figure 1. The channel is described by a conditional probability $P_{y_1, \dots, y_K | x}$ where $x = (x(1), \dots, x(n)) \in \mathcal{X}^n$ denotes the length- n transmitted sequence (codeword) taking value in the input alphabet \mathcal{X} , whereas $y_k = (y_k(1), \dots, y_k(n)) \in \mathcal{Y}_k^n$ denotes the corresponding output sequence at receiver k , taking value in the output alphabet \mathcal{Y}_k . In this multiresolution broadcast setting, we contemplate a *fixed* number of resolution levels (two levels in this example), whereas the number K of served (active) users is typically much larger than the number of resolution levels. In this article, we will limit the analysis to *two* levels: the transmitter seeks to convey a high-priority message $m_H \in \{1, \dots, 2^{nR_H}\}$ to all receiving terminals, as well as—in a *best effort* manner—an optional low-priority message $m_L \in \{1, \dots, 2^{nR_L}\}$ intended for whichever subset of receivers succeeds in decoding it. We say that a rate pair (R_H, R_L) is achievable if with growing n there exists a sequence of encoding and decoding functions (indexed by the blocklength n) such that, for all k ,

$$\lim_{n \rightarrow \infty} \Pr\{\hat{m}_H^{(k)} \neq m_H\} = 0 \quad (3)$$

and for at least one user $k \in \{1, \dots, K\}$,

$$\lim_{n \rightarrow \infty} \Pr\{\hat{m}_L^{(k)} \neq m_L\} = 0. \quad (4)$$

The users satisfying (4) are called *strong users*, whereas the other users, for whom (3) holds but not (4), are referred to as *weak users*. Note that this setting is closely related to (but slightly different from) what in the information-theoretic literature is referred to as the broadcast channel with *degraded message sets*. In fact, in our setup we require an arbitrary non-empty user set (rather than a prescribed user set) to be capable of decoding the low-priority message.

In the following, we shall assume that the channel is memoryless, that is, the channel's conditional probability factorizes as $P_{\mathbf{y}_1, \dots, \mathbf{y}_K | \mathbf{x}}(\mathbf{y}_1, \dots, \mathbf{y}_K | \mathbf{x}) = \prod_{i=1}^n P_{Y_1, \dots, Y_K | X}(y_1(i), \dots, y_K(i) | x(i))$.

A. Orthogonal transmission (OMA)

A simple orthogonal scheme to achieve multiresolution broadcasting is *time division multiplexing* (TDM). This scheme consists in allocating a fraction $\alpha \in [0; 1]$ of transmission time to conveying the high-priority message, while the remaining time is dedicated to transmitting the low-priority message. A rate pair (R_H, R_L) is achievable with this encoding scheme as long as

$$R_H < \min_{k \in \{1, \dots, K\}} \alpha I(X_H; Y_k) \quad (5a)$$

$$R_L < \max_{k \in \{1, \dots, K\}} (1 - \alpha) I(X_L; Y_k). \quad (5b)$$

The minimum and maximum operations are there to ensure, respectively, that all receivers can decode the high-priority message, and that at least one receiver can also decode the low-priority message.

Note that the input variables in (5a)–(5b) are denoted as X_L and X_H , respectively. This is to accommodate the possibility of different signaling distributions depending on the message to be transmitted (m_H or m_L). For example, the messages may be transmitted with a different constellation, or with different powers $E[|X_H|^2] = P_H$ and $E[|X_L|^2] = P_L$ while satisfying a long-term average power constraint $\alpha P_H + (1 - \alpha) P_L \leq P$. We shall refer to this technique as *boost*¹.

Note that in absence of boost, the input variables X_H and X_L are equally distributed (we then denote them both as X) and the achievable rate region only depends on the single-user mutual informations $I(X; Y_k)$.

B. Non-orthogonal transmission (NOMA)

As an alternative to time division multiplexing, a natural candidate among non-orthogonal coding schemes is superposition coding (SC) in combination with successive decoding [19, Theorem 5.2]. One can show that this scheme is capacity-achieving for the multiresolution broadcast problem, in the special case when the channels are mutually degraded.

Let V denote an auxiliary random variable such that $V \leftrightarrow X \leftrightarrow Y_k$ forms a Markov chain for every $k \in \{1, \dots, K\}$. A

rate pair (R_H, R_L) is achievable with superposition coding as long as

$$R_H < \min_{k \in \{1, \dots, K\}} I(V; Y_k) \quad (6a)$$

$$R_L < \max_{k \in \{1, \dots, K\}} I(X; Y_k | V). \quad (6b)$$

One possibility for practically implementing such superposition coding schemes is by a multilevel coded modulation scheme. Consider finite constellation signaling such as, for example, 16-QAM. In the context of MLC with two levels, 4 codeword bits are represented by a 16-ary variable $V = (V_H, V_L)$ that is bijectively mapped to a constellation point $X = \mu(V) = \mu(V_H, V_L)$, wherein V_H and V_L represent the high-priority and the low-priority bits of V , respectively. The splitting of bits between V_H and V_L could be either 1/3, 2/2 or 3/1. The rate pair achievable with MLC corresponds to the special case where in the inequalities (6a)–(6b), the auxiliary V is set to V_H .

IV. THE FAIRNESS–UTILITY TRADEOFF FOR GAUSSIAN MULTIRESOLUTION BROADCASTING

Assume that, conditioned on a complex-valued input symbol $X = x$, the channel output at receiver k is given by

$$Y_k = h_k x + Z_k \quad (7)$$

where $h_k \in \mathbb{C}$ is a channel coefficient, and $Z_k \sim \mathcal{CN}(0, 1)$ is additive white Gaussian noise. Furthermore, assume that the transmitter employs Gaussian random codebooks of power P .

Let us denote the multiplicity of the k -th channel gain as

$$\nu_k = |\{k' : |h_{k'}| = |h_k|\}|. \quad (8)$$

In the Gaussian setting, the single-user channels $P_{Y_k | X}$ are mutually degraded. These degradation relations are strict unless some multiplicities ν_k are larger than one. Let us assume, without loss of generality, that the user indices are ordered such that $|h_1| \geq \dots \geq |h_K|$. Then, they are also ordered by increasing degradation, from $k = 1$ (least degraded) to $k = K$ (most degraded). Consequently, if K_S and $K_W = K - K_S$ denote the number of strong and weak users, respectively, the set of strong users will be $\{1, \dots, K_S\}$ whereas the set of weak users will be $\{K_S + 1, \dots, K\}$.

A. Orthogonal transmission (OMA)

In time division multiplexing, the high-priority stream, encoded at a rate R_H and with a transmit power of $P_H = \frac{\beta}{\alpha} P$, is transmitted during a fraction α of time, whereas the low-priority stream, encoded at a rate R_L and with a transmit power of $P_L = \frac{1-\beta}{1-\alpha} P$, is transmitted during the remaining fraction $1 - \alpha$ of time. The boost parameter β offers us additional flexibility in the power allocation between high- and low-priority data. When optimized, it can potentially improve the achievable tradeoff. If we set $\beta = \alpha$, we have no power boost.

¹We choose this term by analogy to the concept of *reference signal boost* coined in the LTE standard, see also [23] and references therein.

Given a channel gain h_k and parameter pair (α, β) , user k is able to reliably decode the high- and low-priority streams as long as R_H and R_L are smaller than

$$R_H^{(k)}(\alpha, \beta) \triangleq \log_2 \left(1 + |h_k|^2 \frac{\alpha}{\beta} P \right) \quad (9a)$$

$$R_L^{(k)}(\alpha, \beta) \triangleq \log_2 \left(1 + |h_k|^2 \frac{1-\alpha}{1-\beta} P \right) \quad (9b)$$

respectively. The number of strong users K_S , as a function of (α, β, R_L) , is defined as

$$K_S(\alpha, \beta, R_L) = \sum_{k=1}^K \mathbb{1}\{R_L^{(k)}(\alpha, \beta) > R_L\}. \quad (10)$$

Accordingly, the number of weak users is $K_W(\alpha, \beta, R_L) = K - K_S(\alpha, \beta, R_L)$. Since all users should be capable of decoding the high-priority data, we must set R_H to some value smaller than $R_H^{(K)}(\alpha, \beta) = \min_k R_H^{(k)}(\alpha, \beta)$. That is, R_H is constrained by the weakest user. Overall, the users will attain throughputs Q_k given by

$$Q_k = \begin{cases} \alpha R_H + (1-\alpha)R_L & \text{for } k = 1, \dots, K_S \\ \alpha R_H & \text{for } k = K_S + 1, \dots, K. \end{cases} \quad (11)$$

Let us therefore denote the strong- and weak-user throughput as $Q_S = \alpha R_H + (1-\alpha)R_L$ and $Q_W = \alpha R_H$, respectively. According to their definitions in (1)–(2), the fairness and throughput are given respectively by

$$F = \frac{Q_W}{Q_S} \quad (12a)$$

$$U = \frac{Q_W K_W(\alpha, \beta, R_L) + Q_S K_S(\alpha, \beta, R_L)}{K} \quad (12b)$$

and are functions of the parameter tuple $(\alpha, \beta, R_H, R_L)$.

We now turn our attention to the problem of characterizing the optimal tradeoff between F and U , as the parameters α , β , R_H and R_L are varied over all admissible values. This task amounts to computing the supremum of U for every fixed value F' of fairness, which we shall denote as

$$U_{\text{OMA}}^*(F') \triangleq \sup_{\substack{\alpha, \beta, R_H, R_L : \\ F = F'}} U. \quad (13)$$

This function is characterized by the following statement.

Proposition 1 (Gaussian OMA fairness–utility tradeoff): For the time division multiplexing scheme, the optimal fairness–utility tradeoff curve is given by

$$U_{\text{OMA}}^*(F) = \sup_{0 < \beta < 1} \max_k \left\{ \left(1 + \frac{k + \nu_k - 1}{K} \frac{1-F}{F} \right) \times \alpha_k^* R_H^{(K)}(\alpha_k^*, \beta) \right\} \quad (14)$$

where ν_k is defined in (8) and where α_k^* are the unique solutions to equations

$$\begin{aligned} & \left(1 + |h_k|^2 \frac{1 - \alpha_k^*}{1 - \beta} P \right)^{F(1 - \alpha_k^*)} \\ & = \left(1 + |h_K|^2 \frac{\alpha_K^*}{\beta} P \right)^{(1-F)\alpha_K^*}, \quad k = 1, \dots, K. \end{aligned} \quad (15)$$

Proof: The proof is deferred to the Appendix. ■

In absence of power boost, we can simplify (15) by setting $\beta = \alpha_k^*$ (which allows for closed-form solution) and dispense with the supremization over β in (14).

B. Non-orthogonal transmission (NOMA)

In superposition coding, the high- and low-priority streams are encoded at rates R_H and R_L with independent Gaussian codebooks and respective transmit powers $P_H = \gamma P$ and $P_L = (1-\gamma)P$. The resulting high- and low-priority codewords are additively superimposed to produce the transmit sequence

$$\mathbf{x} = \mathbf{x}_H + \mathbf{x}_L. \quad (16)$$

Given a channel gain h_k and power allocation γ , user k is able to reliably decode the high- and low-priority streams as long as their rates R_H and R_L are smaller than

$$R_H^{(k)}(\gamma) \triangleq \log_2 \left(1 + \frac{\gamma |h_k|^2 P}{(1-\gamma) |h_k|^2 P + 1} \right) \quad (17a)$$

$$R_L^{(k)}(\gamma) \triangleq \log_2 (1 + (1-\gamma) |h_k|^2 P) \quad (17b)$$

respectively. The number of strong users K_S , as a function of (γ, R_L) , is defined as

$$K_S(\gamma, R_L) = \sum_{k=1}^K \mathbb{1}\{R_L^{(k)}(\gamma) > R_L\}. \quad (18)$$

Accordingly, the number of weak users is $K_W(\gamma, R_L) = K - K_S(\gamma, R_L)$. Since all users should be able to decode the high-priority stream, we must set $R_H < R_H^{(K)}(\gamma)$. Overall, the users will attain throughputs Q_k given by

$$Q_k = \begin{cases} R_H + R_L & \text{for } k = 1, \dots, K_S \\ R_H & \text{for } k = K_S + 1, \dots, K. \end{cases} \quad (19)$$

Let us therefore denote the strong- and weak-user throughput as $Q_S = R_H + R_L$ and $Q_W = R_H$, respectively. The fairness and throughput are given respectively by (cf. (1)–(2))

$$F = \frac{Q_W}{Q_S} \quad (20a)$$

$$U = \frac{Q_W K_W(\gamma, R_L) + Q_S K_S(\gamma, R_L)}{K} \quad (20b)$$

and are functions of the parameter tuple (γ, R_H, R_L) . We now characterize the optimal tradeoff between F and U as the parameters (γ, R_H, R_L) are varied. Equivalently, we compute the supremum of U for a fixed fairness value $F = F'$, i.e.,

$$U_{\text{NOMA}}^*(F') \triangleq \sup_{\substack{\gamma, R_H, R_L : \\ F = F'}} U. \quad (21)$$

This function is characterized by the following statement.

Proposition 2 (Gaussian NOMA fairness–utility tradeoff): For the superposition coding scheme, the optimal fairness–utility tradeoff curve is given by

$$U_{\text{NOMA}}^*(F) = \max_k \left\{ \left(1 + \frac{k + \nu_k - 1}{K} \frac{1-F}{F} \right) R_H^{(K)}(\gamma_k^*) \right\} \quad (22)$$

where ν_k is defined in (8) and where γ_k^* are the unique solutions to the equations

$$\begin{aligned} & (1 + (1 - \gamma_k^*)|h_k|^2 P)(1 + (1 - \gamma_k^*)|h_K|^2 P)^{\frac{1-F}{F}} \\ & = (1 + |h_K|^2 P)^{\frac{1-F}{F}}, \quad k = 1, \dots, K. \end{aligned} \quad (23)$$

Proof: The proof is deferred to the Appendix. ■

Note that, as one can readily verify by evaluating (14) and (22) (from Propositions 1 and 2, respectively) for the boundary values $F = 0$ and $F = 1$, the extremal points of the tradeoff curves coincide for time division and superposition coding, and are respectively equal to

$$\begin{aligned} U_{\text{OMA}}^*(0) &= U_{\text{NOMA}}^*(0) = \frac{1}{K} \max_k \{ (k + \nu_k - 1) \log_2 (1 + |h_k|^2 P) \} \\ U_{\text{OMA}}^*(1) &= U_{\text{NOMA}}^*(1) = \log_2 (1 + |h_K|^2 P). \end{aligned} \quad (24)$$

C. Crowded cell limits

To reflect a typical situation in downlink channels where distant users have a lower signal-to-noise ratio (SNR) than users located closer to the transmitter, we shall assume that channel gains $|h_k|$ are non-increasing functions of the k -th user's distance from the transmitter.

In a crowded cell, as the number of active users grows large, Proposition 1 can be taken to the limit as $K \rightarrow \infty$. Supposing that the empirical distribution (over the population of receiving terminals) of channel gains $|h|^2$ converges in law to a limiting distribution with support $\mathcal{S} \subset (\sigma_{\min}; +\infty)$ where $\sigma_{\min} > 0$.² This distribution is described by a quantile function³

$$Q(\tau) = \inf \{ \sigma \in \mathcal{S} : \Pr\{|h|^2 \geq \sigma\} \leq \tau \}. \quad (25)$$

By taking the crowded-cell limit of Proposition 1, one can show that the optimal Gaussian OMA tradeoff curve $U_{\text{OMA}}^*(F)$ (cf. (14)–(15)) tends to the limit

$$\begin{aligned} U_{\text{OMA},\infty}^*(F) &= \\ & \sup_{0 < \beta < 1} \max_{0 \leq \tau \leq 1} \left\{ \left(1 + (\tau + \Pr\{|h|^2 = Q(\tau)\}) \frac{1-F}{F} \right) \right. \\ & \quad \times \alpha_\tau^* \log_2 \left(1 + \sigma_{\min} \frac{\alpha_\tau^*}{\beta} P \right) \left. \right\} \end{aligned} \quad (26)$$

where α_τ^* denotes the unique solution to the equation

$$\begin{aligned} & \left(1 + Q(\tau) \frac{1 - \alpha_\tau^*}{1 - \beta} P \right)^{F(1 - \alpha_\tau^*)} \\ & = \left(1 + \sigma_{\min} \frac{\alpha_\tau^*}{\beta} P \right)^{(1-F)\alpha_\tau^*}, \quad 0 \leq \tau \leq 1. \end{aligned} \quad (27)$$

²We exclude zero from the support set to preclude the presence of zero-capacity users which would trivialize the problem, since R_H would have to be set to zero in order to deliver the high-priority stream to all users.

³Sometimes referred to as the inverse complementary cumulative distribution function.

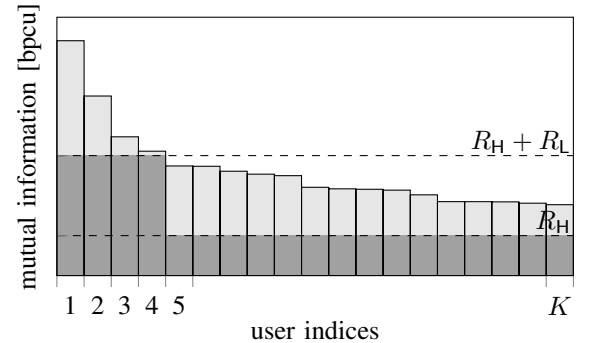
Similarly, by taking the crowded-cell limit of Proposition 2, one can show that the optimal Gaussian NOMA tradeoff curve $U_{\text{NOMA}}^*(F)$ (cf. (22)–(23)) tends to the limit

$$\begin{aligned} U_{\text{NOMA},\infty}^*(F) &= \\ & = \max_{0 \leq \tau \leq 1} \left\{ \left(1 + (\tau + \Pr\{|h|^2 = Q(\tau)\}) \frac{1-F}{F} \right) \right. \\ & \quad \times \log_2 \left(1 + \frac{\gamma_\tau^* Q(\tau) P}{(1 - \gamma_\tau^*) Q(\tau) P + 1} \right) \left. \right\} \end{aligned} \quad (28)$$

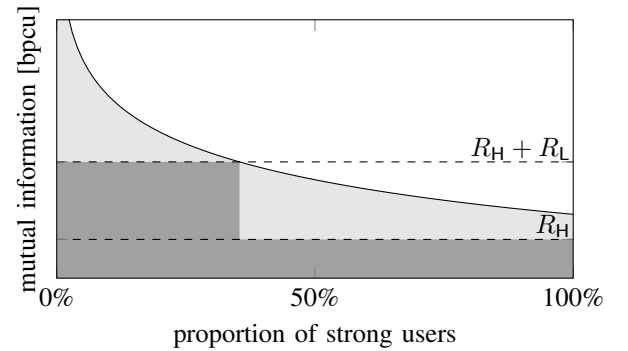
where γ_τ^* denotes the unique solution to the equation

$$\begin{aligned} & (1 + (1 - \gamma_\tau^*) Q(\tau) P)(1 + (1 - \gamma_\tau^*) \sigma_{\min} P)^{\frac{1-F}{F}} \\ & = (1 + \sigma_{\min} P)^{\frac{1-F}{F}}, \quad 0 \leq \tau \leq 1. \end{aligned} \quad (29)$$

Note that if the distribution of $|h|^2$ is absolutely continuous (described by a probability density function), then (26) and (28) are simplified due to $\Pr\{|h|^2 = Q(\tau)\} = 0$ for all $\tau \in [0; 1]$. Likewise, (26) is simplified when discarding boost, by setting $\beta = \alpha_\tau^*$ in (26)–(29) and removing the supremization over β in (26).



(a) Finite number of users K



(b) Crowded-cell limit ($K \rightarrow \infty$)

Fig. 2. Illustration of the fairness–throughput tradeoff in NOMA multiresolution broadcasting: the dark shaded area represents the sum throughput. The channel gain distribution is given by (30).

Figure 2a demonstrates how the NOMA tradeoff characterized in Proposition 2 can be illustrated geometrically: the rate R_L should be ideally increased so as to match the single-user capacity of the weakest user (right-end tail). As to the rate R_H , if throughput is to be maximized, it should be chosen so as to maximize the dark shaded area. Lowering it down from that optimal point will improve fairness at the detriment of average

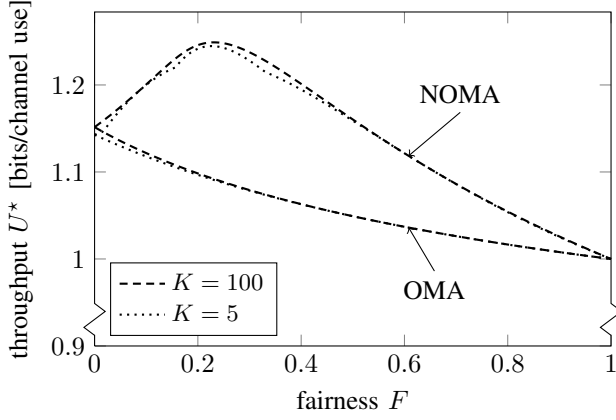


Fig. 3. Fairness-utility tradeoff curves for time division multiplexing $U_{\text{OMA}}^*(F)$ and for superposition coding $U_{\text{NOMA}}^*(F)$. Note that the y -axis is cropped for better visualization. The asymptotic curves $U_{\text{OMA},\infty}^*(F)$ and $U_{\text{NOMA},\infty}^*(F)$ are indistinguishable from the curves corresponding to $K = 100$ and are therefore omitted. The channel gain distribution is given by (30).

throughput. Figure 2b displays the same tradeoff picture, but in the crowded-cell limit, with $U_{\text{NOMA},\infty}^*(F)$ (cf. (26)) in place of $U_{\text{NOMA}}^*(F)$. These figures are similar in spirit to [13, Fig. 2a and 2b], which (in contrast to our Figures 2a–2b) show the analog of this picture in the SNR vs. field strength plane.

The functions $U_{\text{OMA}}^*(F)$ and $U_{\text{NOMA}}^*(F)$ (for exemplary cases with $K = 5$ and $K = 100$ users), as well as their asymptotic limits $U_{\text{OMA},\infty}^*(F)$ and $U_{\text{NOMA},\infty}^*(F)$, are plotted in Figure 3.

D. Numerical simulation

We adopt the 3GPP macro-cell path-loss model in urban areas [24] with an antenna height of 3 m above rooftop, which yields a path-loss exponent of $\lambda = 3.95$. The squared channel amplitude $|h|^2$ is a function of the user's distance d from the base station, of the form $|h|^2 = a(d/d_0)^{-\lambda}$ where $a > 0$ is the channel gain at reference distance $d = d_0$. We choose d_0 to be the a typical cell radius of 500 m, at which the SNR shall be 10 dB, hence $a = 10$.

For simplicity, we shall assume that user locations are statistically independent and uniformly distributed over the circular cell area of radius R . One can show that this uniform location distribution (over the circular cell) induces a distribution of squared channel gains $|h|^2$ described by the quantile function

$$Q(\tau) = a\tau^{-\frac{\lambda}{2}}, \quad \tau \in [0; 1]. \quad (30)$$

V. A PRACTICAL IMPLEMENTATION WITH LTE LDPC CODES AND MULTILEVEL CODING

To illustrate how the NOMA tradeoff dynamics unfold in a more practical implementation, we consider the transmitter and receiver architecture depicted in Figure 4. High-priority and low-priority bit streams are separately encoded by two (possibly different) LDPC encoders whose output bits are piped to serial-to-parallel converters. The four resulting code bits are mapped to a 16-QAM constellation point. For the simulations we have used a set partitioning mapping such

that the 2 high-priority code bits represent the most significant bits in the constellation mapping, whereas the 2 low-priority code bits represent the least significant bits.⁴ We have selected LDPC channel codes [25] with rates $1/5$, $4/9$, $3/5$, $2/3$, $11/15$, $7/9$ and $37/45$ and a common block length $N = 16200$ bits.⁵ High and low-priority messages are encoded with their corresponding rates R_H and R_L into length- N binary codewords $\mathbf{c}^{(H)} = (c_1^{(H)}, \dots, c_N^{(H)})$ and $\mathbf{c}^{(L)} = (c_1^{(L)}, \dots, c_N^{(L)})$, respectively. With 16-QAM, the symbol vector \mathbf{x} that results from mapping these codewords to signal space has length $N/2$. The receiver structure follows a multistage decoding approach, where the demappers differ for the high and low priority messages. For the former, we implement the standard demapper which computes log-likelihood ratios

$$\text{LLR}_{2n-1}^{(H)} = \log \frac{p(y_n | c_{2n-1}^{(H)} = 0)}{p(y_n | c_{2n-1}^{(H)} = 1)} \quad (31a)$$

$$\text{LLR}_{2n}^{(H)} = \log \frac{p(y_n | c_{2n}^{(H)} = 0)}{p(y_n | c_{2n}^{(H)} = 1)} \quad (31b)$$

for $n = 1, \dots, N/2$, where y_n denotes n -th component of vector \mathbf{y} . At the second stage, the demapper exploits the available side information from the previous decoding stage. That is,

$$\text{LLR}_{2n-1}^{(L)} = \log \frac{p(y_n | c_{2n-1}^{(L)} = 0, \hat{c}_{2n-1}^{(H)}, \hat{c}_{2n}^{(H)})}{p(y_n | c_{2n-1}^{(L)} = 1, \hat{c}_{2n-1}^{(H)}, \hat{c}_{2n}^{(H)})}, \quad (32a)$$

$$\text{LLR}_{2n}^{(L)} = \log \frac{p(y_n | c_{2n}^{(L)} = 0, \hat{c}_{2n-1}^{(H)}, \hat{c}_{2n}^{(H)})}{p(y_n | c_{2n}^{(L)} = 1, \hat{c}_{2n-1}^{(H)}, \hat{c}_{2n}^{(H)})}. \quad (32b)$$

These LLR values are then fed to standard LDPC decoders for recovering the high and low priority message, respectively.

For each data stream, we require a packet error probability below 10^{-2} and choose freely among rates $1/5$, $4/9$, $3/5$, $2/3$, $11/15$, $7/9$ and $37/45$. Given a cell-edge SNR of 10 dB, our simulations reveal that in order to achieve an error probability of at most 10^{-2} , the high-priority stream can be encoded at any of these available rates except the highest rate $37/45$. Each of the six remaining high-priority encoders is then combined with any of the seven low-priority encoders, yielding the six curves plotted in Figure 5. The resulting points are connected by solid black curves (one curve per high-priority encoder, seven points per curve). In addition, we have plotted in gray the curves obtained from running through all TDM combinations between the two operating points corresponding to the endpoints of each of the solid black curves. As a result, for the practical LDPC implementation we obtain a collection of NOMA–OMA curve pairs (in black and gray, respectively) that are directly comparable to their theoretical counterparts obtained with random Gaussian codes in Figure 3. The throughput U^* is computed based on the channel gain distribution (30) from Subsection IV-D and an infinite number of users ($K \rightarrow \infty$).

⁴This choice is heuristic and not guided by any notion of optimality. Varying the constellation mapping and the dimensions of S/P converters may produce many more (and possibly better) points on the F – U plane.

⁵Having codewords of equal length eases the implementation, especially for mapping and demapping tasks.

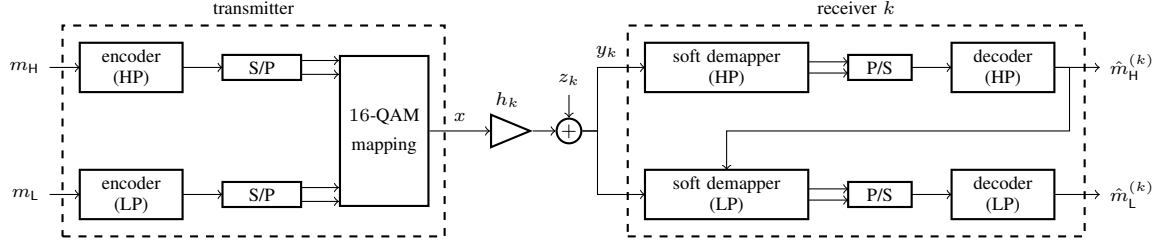


Fig. 4. Transmit and receive architecture for a superposition coding scheme based on LDPC codes and multilevel coded modulation with two levels: high priority (HP) and low priority (LP)

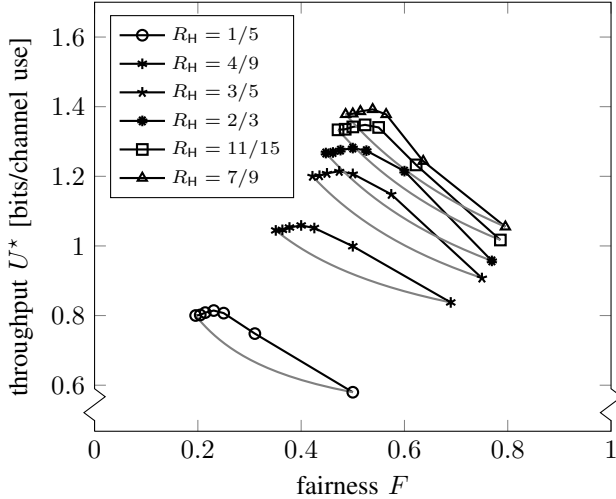


Fig. 5. Fairness-utility tradeoff curves for LTE LDPC codes and superposition coding based on multilevel coding with a set partition mapping. The OMA baseline curve corresponding to each NOMA curve is plotted in gray. Note that the y -axis is cropped for better visualization.

We clearly observe the same trend as in the NOMA scheme from Figure 3: unlike the OMA scheme which exhibits a clear tension between fairness and utility on the entire range of achievable values, in the case of NOMA the utility (throughput) passes through a maximum before redescending to its minimum value as the fairness sweeps from zero to one.

VI. CONCLUSION

We have introduced a framework to characterize the tension that exists between user fairness and sum utility in multiresolution broadcast settings. We have demonstrated that there exists a *tradeoff* between these two metrics, in contrast to the private-message broadcast setting, where the sum-rate maximizing point tends to be maximally unfair. In the OMA scheme, this F - U tradeoff covers the entire range of fairness and utility values, while in the NOMA scheme, it is limited to fairness values above a utility-maximizing threshold value.

While this initial study treats a simple setting, we expect the general trend to persist in more general settings, which are left for future research. These include, for instance, multiresolution with more than two layers, multiple antennas, a non-identity function g , variations of the fairness metric, or different coded modulation schemes such as bit-interleaved coded modulation or hierarchical coding for unequal error protection.

APPENDICES

PROOF OF PROPOSITION 1

Since R_H is constrained to being smaller than $R_H^{(K)}(\alpha, \beta)$ and since on the other hand, both F and U as given in (12a)–(12b) are non-decreasing and continuous in R_H , we can replace R_H with $R_H^{(K)}(\alpha, \beta)$ in (12a)–(12b) for the purpose of computing the supremum $U_{\text{OMA}}^*(F)$. Next, we observe that by fixing the fairness ratio $\alpha R_H^{(K)}(\alpha, \beta) / (\alpha R_H^{(K)}(\alpha, \beta) + (1 - \alpha)R_L)$ to the value $F' > 0$, we are imposing that the parameter triple (α, β, R_L) satisfy the relationship

$$R_L = \left(\frac{1}{F'} - 1 \right) \frac{\alpha}{1 - \alpha} R_H^{(K)}(\alpha, \beta) \quad (33)$$

such that in (12b), R_L can be replaced by the right-hand side of (33). The supremum throughput for a target fairness $F' > 0$ can thus be expressed as

$$U_{\text{OMA}}^*(F') = \frac{1}{K} \sup_{0 < \beta < 1} \max_{0 \leq \alpha \leq 1} \left\{ K \alpha R_H^{(K)}(\alpha, \beta) + K_S \left(\alpha, \beta, \frac{(1 - F')\alpha}{F'(1 - \alpha)} R_H^{(K)}(\alpha, \beta) \right) \frac{1 - F'}{F'} \alpha R_H^{(K)}(\alpha, \beta) \right\}. \quad (34)$$

Note that for a fixed β , the K_S term is piecewise constant, integer-valued, right-continuous and non-increasing in α . It takes value K at $\alpha = 0$ and decreases as a staircase function down to 0 at α approaching 1 (from the left). On any open interval on which said term is constant, the argument of the inner maximum (34) is an increasing function of α because $R_H^{(K)}(\alpha, \beta)$ is increasing in α . Hence, on that open interval, the function has no local maximum, so the inner maximum in (34) must be attained at (the left limit of) one of the jump discontinuities of the K_S term. The locations $\alpha_1^*, \dots, \alpha_K^*$ of these discontinuities can be determined by solving the following equations in α (for each $k = 1, \dots, K$):

$$R_L^{(k)}(\alpha, \beta) = \frac{(1 - F')\alpha}{F'(1 - \alpha)} R_H^{(K)}(\alpha, \beta). \quad (35)$$

Upon inserting (9a)–(9b), these equations can be written as

$$\left(1 + |h_k|^2 \frac{1 - \alpha}{1 - \beta} P \right)^{F'(1 - \alpha)} = \left(1 + |h_K|^2 \frac{\alpha}{\beta} P \right)^{(1 - F')\alpha}. \quad (36)$$

In absence of power boost ($\beta = \alpha$), this simplifies to

$$(1 + |h_k|^2 P)^{F'(1 - \alpha)} = (1 + |h_K|^2 P)^{(1 - F')\alpha} \quad (37)$$

which can be solved in closed form, yielding solutions

$$\frac{\alpha_k^*}{1 - \alpha_k^*} = \frac{F' \log_2(1 + |h_k|^2 P)}{1 - F' \log_2(1 + |h_K|^2 P)}. \quad (38)$$

Since $|h_k|$ are non-increasingly ordered, it clearly follows that the values α_k^* are non-increasingly ordered too.

Since the K_S term equals $k + \nu_k - 1$ when α lies in the left-hand neighborhood of α_k^* , we can replace K_S with $k + \nu_k - 1$ in (34) for the purpose of computing the maximum. Thus, the maximization reduces to a finite search over the discontinuities α_k^* , i.e.,

$$U_{\text{OMA}}^*(F') = \max_k \left\{ \left(1 + (k + \nu_k - 1) \frac{1 - F'}{K F'} \right) \times \alpha_k^* R_{\text{H}}^{(K)}(\alpha_k^*, \beta) \right\} \quad (39)$$

which concludes the proof.

PROOF OF PROPOSITION 2

The reasoning is similar to the proof of Proposition 1. Due to the requirement that even the weakest user should be able to decode the high-priority stream, R_{H} is constrained to $[0; R_{\text{H}}^{(K)}(\gamma))$ for any $\gamma \in [0; 1]$. In addition, both F and U as given in (20a)–(20b) are monotone in R_{H} , hence we can replace R_{H} with $R_{\text{H}}^{(K)}(\gamma)$ in (20a)–(20b) for the purpose of determining the supremum $U_{\text{NOMA}}^*(F')$. Next, we observe that by fixing the fairness ratio $R_{\text{H}}^{(K)}(\gamma)/(R_{\text{H}}^{(K)}(\gamma) + R_{\text{L}})$ to the value $F' > 0$, we lock the parameters γ and R_{L} into a one-to-one relationship

$$R_{\text{L}} = \left(\frac{1}{F'} - 1 \right) R_{\text{H}}^{(K)}(\gamma) \quad (40)$$

such that in (20b), R_{L} can be replaced by the right-hand side of (40). The supremum throughput for a target fairness $F' > 0$ can thus be expressed as

$$U_{\text{NOMA}}^*(F') = \frac{1}{K} \max_{0 \leq \gamma \leq 1} \left\{ K R_{\text{H}}^{(K)}(\gamma) + K_S \left(\gamma, \frac{(1 - F') R_{\text{H}}^{(K)}(\gamma)}{F'} \right) \frac{(1 - F') R_{\text{H}}^{(K)}(\gamma)}{F'} \right\}. \quad (41)$$

Note that the K_S term is piecewise constant, integer-valued, right-continuous and non-increasing in γ , because it is non-increasing in both the first and second argument. It takes value K at $\gamma = 0$ and decreases as a staircase function down to 0 at $\gamma = 1$. On any open interval on which this term is constant, the argument of the maximum (41) is an increasing function of γ because $R_{\text{H}}^{(K)}(\gamma)$ is increasing in γ . Hence, on that open interval, the function exhibits no local maxima, so the maximum (41) must be attained at (the left-hand limit of) one of the jump discontinuities of the K_S term. The locations $\gamma_1^*, \dots, \gamma_K^*$ of these discontinuities can be determined by solving the following equations in γ (for $k = 1, \dots, K$):

$$R_{\text{L}}^{(k)}(\gamma) = \frac{(1 - F') R_{\text{H}}^{(K)}(\gamma)}{F'}. \quad (42)$$

Inserting (17a)–(17b) and after some algebra, these equations can be written as

$$(1 + (1 - \gamma)|h_k|^2 P)(1 + (1 - \gamma)|h_K|^2 P)^{\frac{1 - F'}{F'}} = (1 + |h_K|^2 P)^{\frac{1 - F'}{F'}}. \quad (43)$$

Clearly, since $|h_k|$ are non-increasingly ordered, it follows that the solutions γ_k^* of the equations (43) are non-increasingly ordered too.

Since the K_S term takes the value $k + \nu_k - 1$ at the left-hand side of γ_k^* , we can replace it with $k + \nu_k - 1$ in (41) and reduce the maximization to a finite search over the discontinuities γ_k^* , i.e.,

$$U_{\text{NOMA}}^*(F') = \max_k \left\{ \left(1 + (k + \nu_k - 1) \frac{1 - F'}{K F'} \right) R_{\text{H}}^{(K)}(\gamma_k^*) \right\} \quad (44)$$

which concludes the proof.

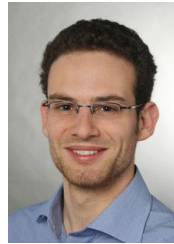
ACKNOWLEDGMENT

This work was supported by the Catalan Government under grant 2017 SGR 1479 and by the Spanish Ministry of Economy and Competitiveness through project TEC2014-59255-C3-1-R (ELISA).

REFERENCES

- [1] T. Cover, "Broadcast channels," *IEEE Transactions on Information Theory*, vol. 18, no. 1, pp. 2–14, Jan. 1972.
- [2] R. G. Gallager, "Capacity and coding for degraded broadcast channels," *Probl. Peredachi Inf.*, vol. 10, no. 3, pp. 3–14, 1974.
- [3] P. Bergmans, "Random coding theorem for broadcast channels with degraded components," *IEEE Transactions on Information Theory*, vol. 19, no. 2, pp. 197–207, Mar. 1973.
- [4] H. Weingarten, Y. Steinberg, and S. S. (Shitz), "The capacity region of the Gaussian multiple-input multiple-output broadcast channel," *IEEE Transactions on Information Theory*, vol. 52, no. 9, May 2006.
- [5] M. Salman and M. K. Varanasi, "On the capacity region of the k-user discrete memoryless broadcast channel with two degraded messages," in *IEEE International Symposium on Information Theory (ISIT)*, Jun. 2017, pp. 1048–1052.
- [6] Y. Saito, Y. Kishiyama, A. Benjebbour, T. Nakamura, A. Li, and K. Higuchi, "Non-orthogonal multiple access (NOMA) for cellular future radio access," in *IEEE 77th Vehicular Technology Conference (VTC Spring)*, Jun. 2013, pp. 1–5.
- [7] 3GPP, "Study on downlink multiuser superposition transmission (MUST) for LTE (Re.13)," 3rd Generation Partnership Project (3GPP), TR 36.859, Dec. 2015. [Online]. Available: <http://www.3gpp.org>
- [8] U. Wachsmann, R. F. H. Fischer, and J. B. Huber, "Multilevel codes: Theoretical concepts and practical design rules," *IEEE Transactions on Information Theory*, vol. 45, no. 5, pp. 1361–1391, Jul. 1999.
- [9] S. Pfletschinger, M. Navarro, and C. Ibars, "Multilevel coding for non-orthogonal broadcast," in *48th Asilomar Conference on Signals, Systems and Computers*, Nov. 2014.
- [10] L. Dai, B. Wang, Y. Yuan, S. Han, C. I. I., and Z. Wang, "Non-orthogonal multiple access for 5G: solutions, challenges, opportunities, and future research trends," *IEEE Communications Magazine*, vol. 53, no. 9, pp. 74–81, Sep. 2015.
- [11] L. Zhang, W. Li, Y. Wu, X. Wang, S. Park, H. M. Kim, J.-Y. Lee, P. Aguilera, and J. Montalban, "Layered division multiplexing: Theory and practice," *IEEE Transactions on Broadcasting*, vol. 62, no. 2, pp. 216–232, Mar. 2016.
- [12] ATSC, "ATSC Standard: Physical Layer Protocol (A/322)," Advanced Television Systems Committee (ATSC), A 322:2017, Jun. 2017. [Online]. Available: <https://www.atsc.org/wp-content/uploads/2016/10/A322-2017a-Physical-Layer-Protocol-1.pdf>

- [13] L. Zhang, Y. Wu, W. Li, K. Salehian, S. Lafleche, X. Wang, S. I. Park, H. M. Kim, J. y. Lee, N. Hur, P. Angueira, and J. Montalban, "Layered-division multiplexing: An enabling technology for multicast/broadcast service delivery in 5G," *IEEE Communications Magazine*, vol. 56, no. 3, pp. 82–90, Mar. 2018.
- [14] S. Timotheou and I. Krikidis, "Fairness for non-orthogonal multiple access in 5G systems," *IEEE Signal Processing Letters*, vol. 22, no. 10, pp. 1647–1651, Oct. 2015.
- [15] J. Körner and K. Marton, "General broadcast channels with degraded message sets," *IEEE Transactions on Information Theory*, vol. 23, no. 1, pp. 60–64, Jan. 1977.
- [16] C. Nair and M. Yazdanpanah, "Sub-optimality of superposition coding region for three receiver broadcast channel with two degraded message sets," in *IEEE International Symposium on Information Theory (ISIT)*, Jun. 2017, pp. 1038–1042.
- [17] K. Marton, "A coding theorem for the discrete memoryless broadcast channel," *IEEE Transactions on Information Theory*, vol. 25, no. 3, pp. 306–311, May 1979.
- [18] E. Ekrem and S. Ulukus, "An outer bound for the Gaussian MIMO broadcast channel with common and private messages," *IEEE Transactions on Information Theory*, vol. 58, no. 11, pp. 6766–6772, Nov. 2012.
- [19] A. El Gamal and Y.-H. Kim, *Network Information Theory*. New York, USA: Cambridge University Press, 2012.
- [20] Z. Ding, M. Peng, and H. V. Poor, "Cooperative non-orthogonal multiple access in 5G systems," *IEEE Communications Letters*, vol. 19, no. 8, pp. 1462–1465, Aug. 2015.
- [21] Z. Wei, J. Guo, D. W. K. Ng, and J. Yuan, "Fairness comparison of uplink NOMA and OMA," in *IEEE 85th Vehicular Technology Conference (VTC Spring)*, June 2017, pp. 1–6.
- [22] T. Lan, D. Kao, M. Chiang, and A. Sabharwal, "An axiomatic theory of fairness in network resource allocation," in *IEEE International Conference on Computer Communications (INFOCOM)*, Mar. 2010.
- [23] A. Lozano, "Interplay of spectral efficiency, power and Doppler spectrum for reference-signal-assisted wireless communication," *IEEE Transactions on Wireless Communications*, vol. 7, no. 12, pp. 5020–5029, Dec. 2008.
- [24] 3GPP, "Evolved Universal Terrestrial Radio Access (E-UTRA); Further advancements for E-UTRA physical layer aspects," 3rd Generation Partnership Project (3GPP), TS 36.814. [Online]. Available: <http://www.3gpp.org/ftp/specs/html-info/36814.htm>
- [25] "Digital Video Broadcasting (DVB); Frame structure channel coding and modulation for a second generation digital terrestrial television broadcasting system (DVB-T2)," European Telecommunications Standards Institute, Sophia-Antipolis, FR, Standard, 2011.



Adriano Pastore (S'10–M'14) is a researcher at the Department for Statistical Inference for Communications and Positioning at the Centre Tecnològic de Telecomunicacions de Catalunya (CTTC) in Castelldefels, Spain. He received his Ph.D. (with highest distinction) from the Signal Theory and Communications Department of the Universitat Politècnica de Catalunya (UPC) in 2014, the Diplôme d'Ingénieur from the Ecole Centrale Paris and the Dipl.-Ing. in electrical engineering from the Technical University of Munich in 2009. Between 2014 and 2016, he was a postdoctoral fellow at the School of Computer and Communication Sciences at École Polytechnique Fédérale de Lausanne, Switzerland. His research interests include network information theory, wireless communications, privacy and machine learning.



Monica Navarro (S'96, M'98, SM'08) Dr. Monica Navarro is the Head of the Communication Systems Division and Senior Researcher at the Centre Tecnològic de Telecomunicacions de Catalunya within the Communication Systems Division. She received the MSc degree in Telecommunications Engineering from Universitat Politècnica de Catalunya in 1997 and the PhD degree in Telecommunications from the Institute for Telecommunications Research (ITR), University of South Australia, in 2002. From Oct. 1997 to Dec. 1998 she was a Research Assistant at the Department of Signal Theory and Communications at the UPC, where she worked on the development of fractal shape multiband antennas for wireless cellular communications systems. She has also been part-time lecturer at the Universitat Pompeu Fabra, Barcelona. Her primary areas of interest are on information processing with applications to wireless communications and positioning. Particularly on iterative information processing, adaptive transmissions, coding techniques and random access protocols for massive access. She has strong expertise on new radio air interfaces for cellular networks. Over the last 10 years she has lead projects funded by the European Commission, Spanish and Catalan Governments, as well as the European Space Agency (ESA). She served at the Editorial Board of Emerging Telecommunications Technologies (ETT) from 2013 to 2016.